15

Corrosion Performance and Tribological Properties of Carbonitrided 304 Stainless Steel

A.M. Abd El-Rahman[1,2], F.M. El-Hossary[1], F. Prokert[2], N.Z. Negm[1], M.T. Pham[2] and E. Richter[2]
[1]*Physics Department, Faculty of Science, South Valley University, Sohag Branch, Sohag,*
[2]*Institut für Ionenstrahlphysik und Materialforschung, Helmholtz-Zentrum Dresden-Rossendorf,*
[1]*Egypt*
[2]*Germany*

1. Introduction

In general, the solid solution austenitic phase (γ) with high chromium content (12 % - 20 %) is responsible about the excellent corrosion performance of austenitic alloys. This advantage allows these alloys to use in biomedical, food and chemical, pulp and paper chemical, petrochemical, heat exchange and nuclear power plant industries [1-4]. However, most of these applications are suffering from their relatively low hardness and poor tribological properties.

Various surface modification technologies such as nitriding, carburizing and nitrocarburizing are used to improve the mechanical and tribological properties of austenitic stainless steels [5-12]. In most cases an increase in surface hardness is accompanied by a decrease in corrosion resistance [13]. The decrease in the corrosion resistance is caused by heavy precipitations of chromium carbide and chromium nitride on the grain boundaries, which are surrounded by chromium-depleted zones [14]. More investigations are succeeded to maintain and sometimes to improve the corrosion resistance of stainless steels after nitriding [15-16]. It is well known that the formation of nitrogen supersaturated solid solution phase without CrN precipitations should maintain the good corrosion resistance of stainless steel [5, 17].

In this paper we present the effect of N_2 to C_2H_2 gas pressure ratio on the corrosion performance and tribological properties of AISI 304 austenitic stainless steel after rf plasma carbonitriding at a relatively low pressure.

2. Experimental work

The samples were treated at a fixed input plasma power of 450 W and for a processing time of 10 min. The gas pressure related to N_2/C_2H_2 ratio was varied from 100% N_2 to 100% C_2H_2. The pressure was increased from an atypical base pressure of 1.3×10^{-2} mbar to a total gas pressure

of 8.4x10-2 mbar. The sample was heated mainly by the rf field. The sample temperature was measured during the rf plasma process by a Chromel-Alumel thermocouple, attached to the sample holder. As shown in Fig. 1, the substrate temperature was influenced by the effect of gas compositions. It was found that the temperature gradually increases from 475 ˚C for pure nitriding up to 550 ˚C for carbonitriding (50% C_2H_2, 50% N_2) and raises up to 600 ˚C for pure carburizing. Grazing incidence X-ray diffraction (GIXRD) with Cu Kα radiation was used to determine the phases, present in the treated layers. For the chosen incidence angle of 2° the (1/e)-penetration depth of the X-rays was approximately 700 nm. The recorded diffraction pattern shows therefore mainly the structure of the phases formed in this near-surface region. In this paper we concentrate on the study of corrosion resistance, surface morphology before and after corrosion, and tribological properties of the treated samples. The surface roughness was measured by use of the rough machine (Dektak 8000, Veeco Instrument GmbH). Wear and friction measurement were performed at room temperature in laboratory air with low humidity of 16 to 24 % using an oscillating ball-on-disk type tribometer wear tester without lubrication. The 3-mm ball of cobalt tungsten carbide was moved at mean sliding speed of 15 mm/sec with different normal loads of 3, 5 and 8 N. The corrosion properties were evaluated using the electrochemical testing technique. The corrosion tests were performed in a 1 wt. % NaCl solution by application of the potentiodynamic polarization method. A three-electrode electrochemical cell has been used, counter and reference electrode were related to Pt and saturated calomel electrode, respectively.

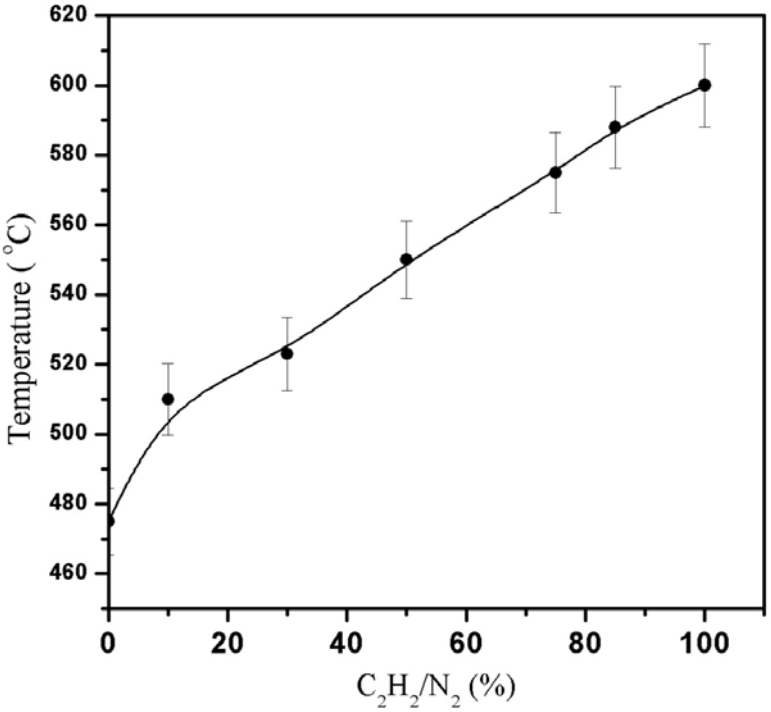

Fig. 1. Temperature variation as a function of the gas composition.

The anodic polarization curves were recorded with potential scan rate of 10 mV /sec. The potentiodynamic polarization curve is plotted using AutoLab PGSTAT 12 + GPES software. The surface morphology before and after corrosion tests and the chemical composition of selected parts of the as-prepared layers were examined by scanning electron microscopy (SEM) and energy dispersive X-ray analysis (EDAX), respectively.

3. Results

3.1 Phase formation

The microstructure of the untreated sample and samples treated at different gas compositions (N_2/C_2H_2) obtained by GIXRD have been studied by us before [11] and it is shown in Fig. 2. It is briefly described here to correlate tribological and corrosion results to the microstructure of the modified surface layers. Only fcc austenitic stainless steel (γ) and bcc ferritic iron (α) were detected in the untreated sample. After treatment at 100 % N_2, the Fe_2N and CrN phases are observed. The formation of CrN phase is typical for such a high treatment temperature (475 °C). Residual signals from fcc γ-austenite and bcc ferritic iron are present. At high percentage of nitrogen (90 %) iron nitride phases of Fe_2N, Fe_3N and chromium nitride phase CrN are detected beside the main phase/phases, cubic Fe_4N and/or nitrogen-expanded austenite (γ_n). Due to an overlapping of the strong reflections, the existence of both phases is possible. The intensities of the CrN are lower in comparison to the case of pure nitriding. This might be due to nitrogen atoms, which are dissipated in favor of the formation of the iron nitrides (Fe_3N, Fe_4N) and γ_n phases. In the sample treated at high carbon content (75 % C_2H_2 and 25 % N_2), most of the peaks are correlated to Fe_3C, carbon-expanded austenite (γ_c) beside the CrN phase. For the sample treated at 100 % C_2H_2, the γ_c and CrC phases are only detected.

3.2 Surface roughness

Fig. 3 shows the relative surface roughness, determined by the ratio of the roughness of treated samples to untreated one, as a function of different C_2H_2/N_2 gas pressure ratios. The value of the surface roughness of the untreated sample was 46.3 nm. Due to pure nitriding the surface roughness is increased only by a factor of 1.33. By addition of C_2H_2, the surface roughness increases abruptly up to a maximum value of 4.12, reached at 30 % C_2H_2. The value is nearly the same up to a gas content of 50 % C_2H_2 and decreases significantly for samples treated at high carbon content (75 % C_2H_2) and at pure carburising.

3.3 Wear test and friction coefficient

The friction coefficient is a mechanical parameter, which depends on the surface material composition and the nature of the surface itself. Fig. 4 presents the relative friction coefficient for the samples treated at different gas composition. It relates the friction coefficient of the treated sample to the value of the untreated stainless steel (0.78). The measurement of the friction coefficient has been done for different number of tracks. For pure nitriding, after the first 2000 tracks, at which the wear depth is lower than 0.6 µm, in all examined treated samples, the friction coefficient is reduced to 59 %. While the C_2H_2/N_2 gas ratio increases, the values of the friction coefficient decrease significantly and reaching approximately 14 % for pure carburizing. As a function of gas composition, the friction

coefficient for 20000 numbers of tracks has nearly the same values. This reveals the homogeneity and the mechanical stability of the microstructure of the treated layer within the examined range in the near surface region.

The sliding wear behaviour of the untreated and treated samples was assessed using oscillating ball-on-disk type tribometer. The depth of the wear tracks of examined samples as a function of wear path at a load of 3 N is shown in Fig. 5. Generally, the wear resistance of the untreated samples in comparison to the treated is extremely poor. For all treated samples, examined up to 320 m wear path, maximum one micrometer wear depth has been observed and the wear depth slowly increases with increasing wear path. Otherwise the wear rates have been accounted as total volume loss in mm^3 divided by the total sliding distance in meters. The wear rates for the untreated material were accounted in order to know the improvement in the wear rates for treated one. The wear rate for the untreated 304 austenitic stainless steel was 2.4×10^{-4} mm^3/m at 20000 numbers of tracks (80 m wear path).

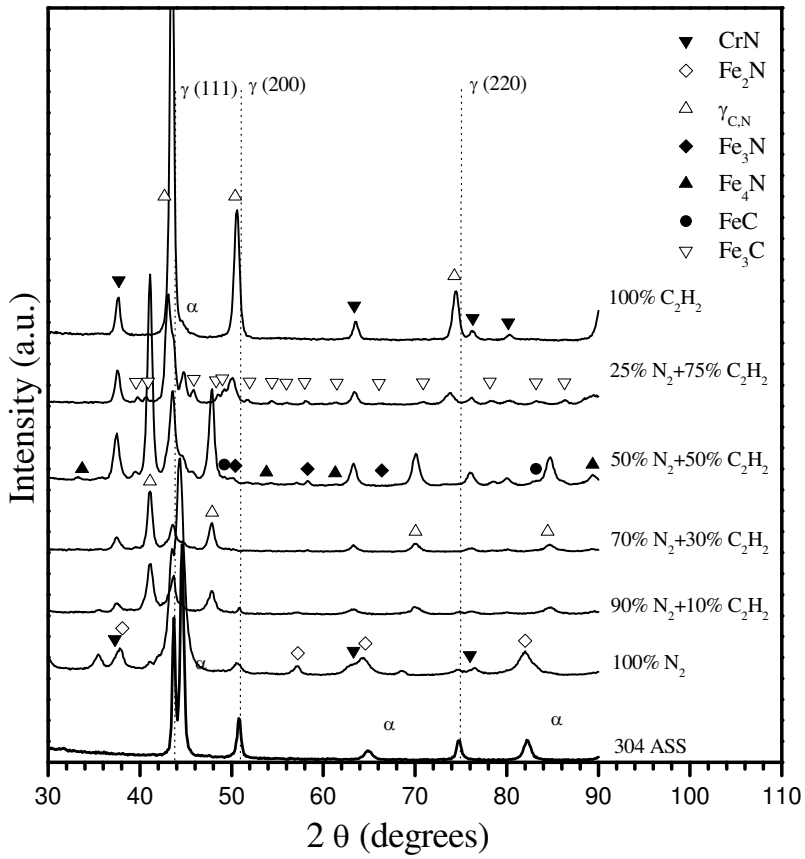

Fig. 2. X-ray diffraction pattern obtained at 2° grazing incidence from 304 stainless steel of untreated samples and samples treated at different C_2H_2/N_2 gas pressure ratios.

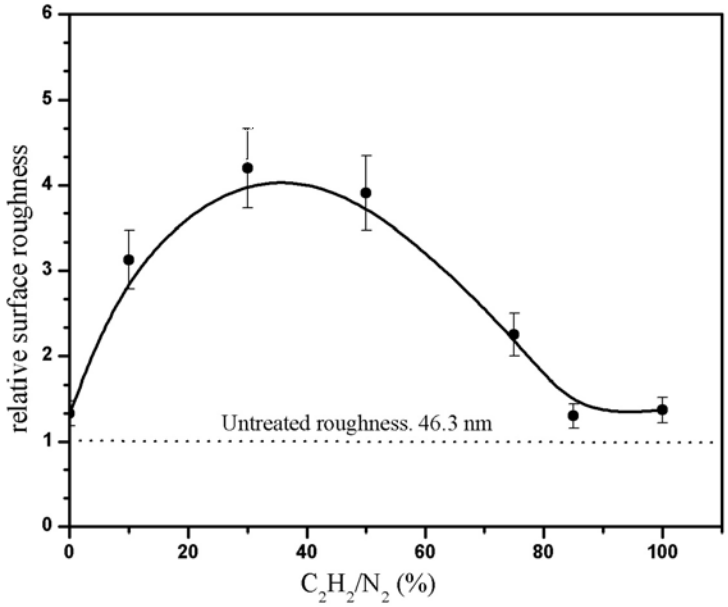

Fig. 3. Relative surface roughness for 304 ASS samples treated at different C_2H_2/N_2 gas ressure ratios.

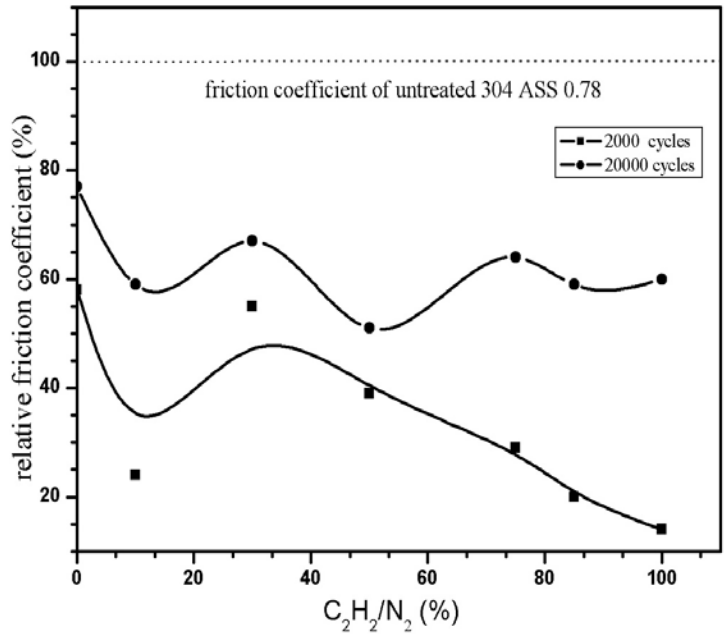

Fig. 4. Relative coefficient of friction as a function of gas composition at different number of cycles.

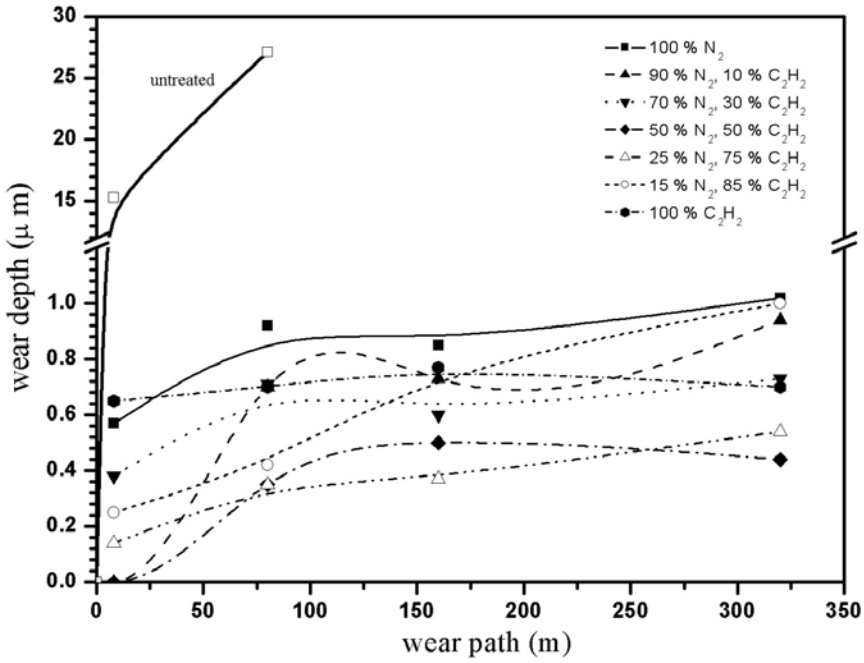

Fig. 5. Wear depth of treated samples at different gas composition compared to an untreated sample.

Fig. 6 presents the variation in the wear rate at different number of tracks as a function of gas composition ratios for a load of 3 N. The wear rate after treatment was reduced by more than two orders in comparison with the untreated material. At 20000 wear tracks, a decrease of the wear rate was observed as much as the C_2H_2 gas ratio increases. However, this improvement was continued up to 75 % C_2H_2 and 50 % C_2H_2 at 40000 and 80000 numbers of tracks, respectively. The decrease in the wear rate by increasing the C_2H_2 content is related to some improvement in the friction coefficient of treated layers due to fine carbon precipitations which work as solid lubricant on the first few hundred nanometers. However, for samples treated at high carbon content, a small increase in the wear rate can be seen with increasing the sliding distance.

Fig. 7 shows the resistance of treated samples toward physical wearing by accounting the wear rate at different loads of 3 N, 5 N and 8 N. The wear rate of untreated sample is increased by one order from 2.7 x 10^{-4} mm^3/m to 2.7 x 10^{-3} mm^3/m at 5 N and 8 N, respectively. Generally, for all treated samples the wear rate increases in the same order with the load. The wear rate decreases significantly with the increase of the C_2H_2/N_2 gas ratio and for relatively high load (8 N) it reaches a minimum at 50 %.

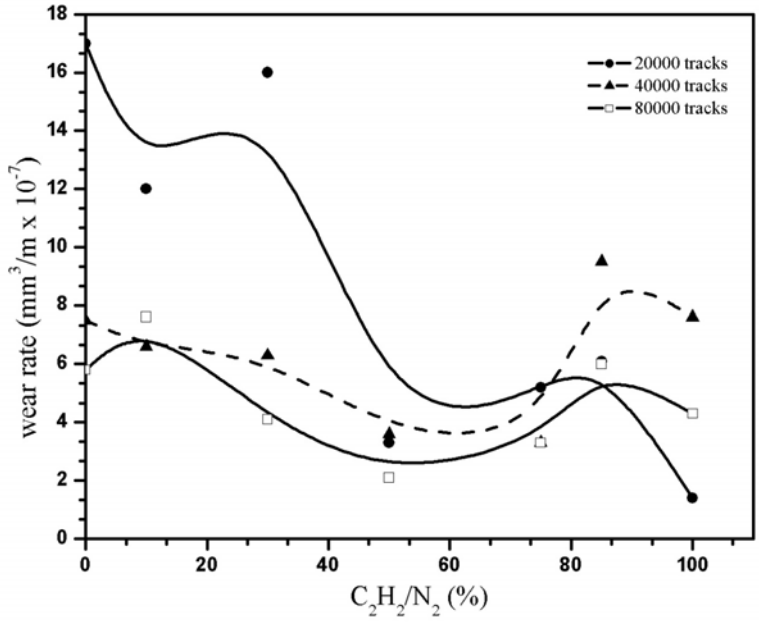

Fig. 6. Wear rate of treated samples as a function of gas composition for a load of 3 N.

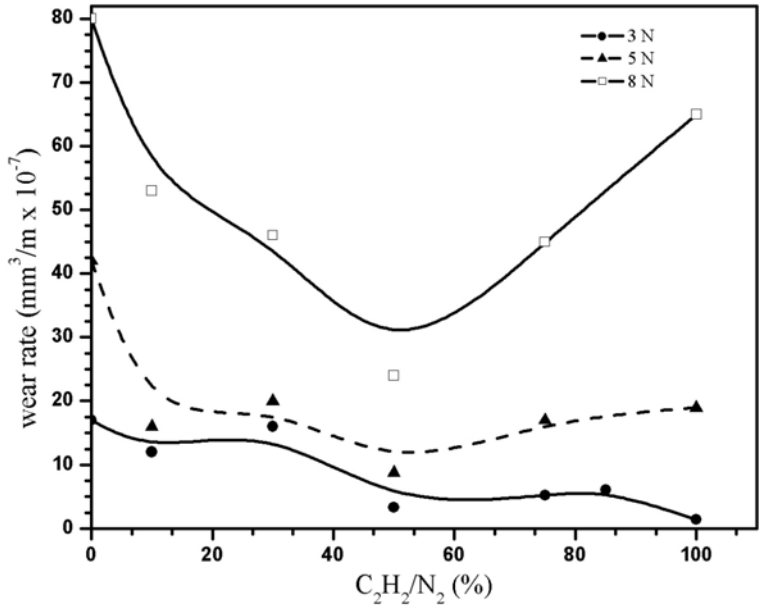

Fig. 7. Wear rate of treated samples as a function of gas composition at different loads and fixed numbers of tracks (200000).

3.4 Corrosion test and surface morphology

Fig. 8 shows the anodic polarization curves obtained from treated and untreated 304-AISI samples. These results was published elsewhere and represented here to make a correlation to the study of the surface morphology before and after corrosion effect [12]. The increase in the corrosion current and decrease in corrosion potential indicate a degradation of the corrosion resistance for the treated samples. The highest degradation in comparison to the untreated sample is observed for the sample treated in pure nitrogen and carbon plasma. The lowest degradation in the corrosion resistance is observed for the sample treated at the gas composition of 70 % N_2 and 30 % C_2H_2.

The SEM pictures, given in Fig. 9, show the surface morphology of the untreated in comparison to treated samples. Moreover the treated surfaces have been scanned after corrosion test. The original material (304-AISI) may be characterized by a non-uniform shapes, thin grain boundaries and very weak links between the grains. In general the treated samples have wider grain boundaries and smaller grain size. Nitrocarburized samples show also a tendency of grain coalescence. At preparation with 100 % C_2H_2, the grain boundaries are not clearly visible, which is caused by the higher carbon precipitations at the surface. However, it seems that the grain size is larger than that obtained in the nitrocarburized samples.

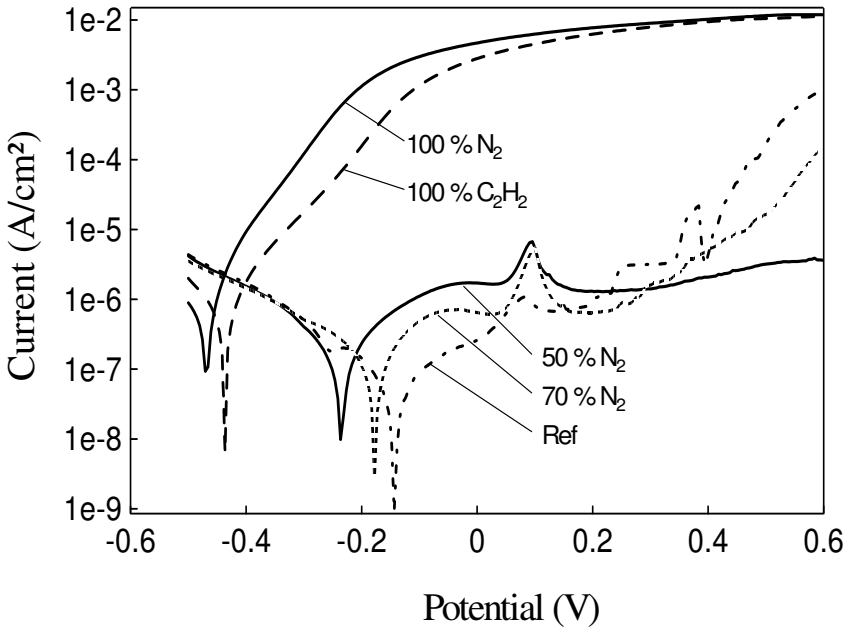

Fig. 8. Anodic polarization curves for untreated and treated samples at different C_2H_2/N_2 gas pressure ratios obtained in 1 wt. % NaCl solution.

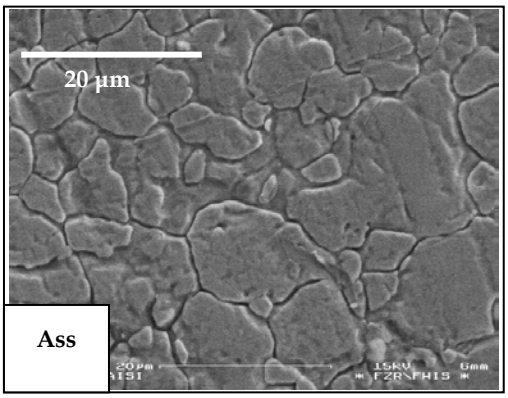
20 µm
Ass

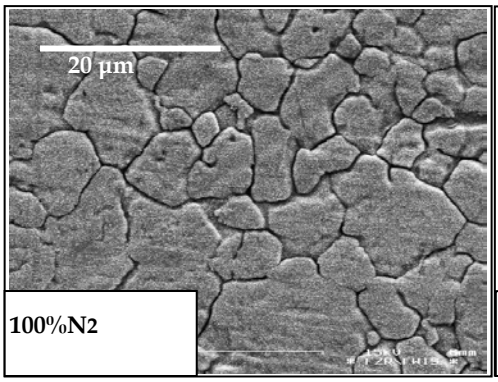
20 µm
100%N2

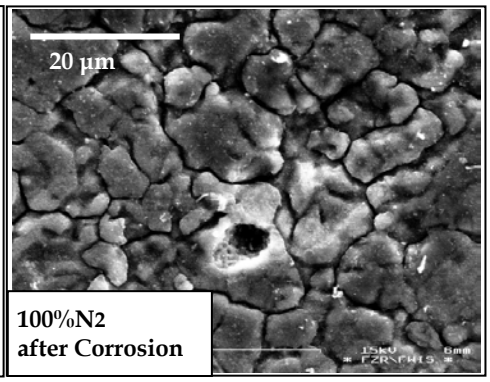
20 µm
100%N2
after Corrosion

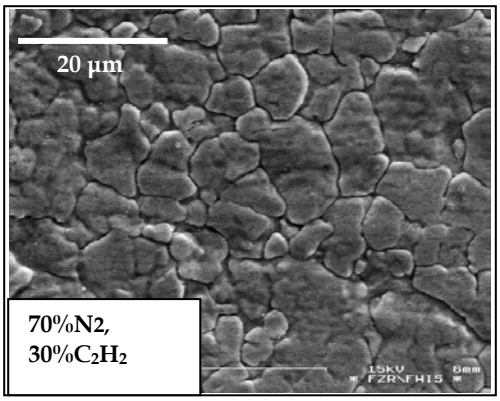
20 µm
70%N2,
30%C2H2

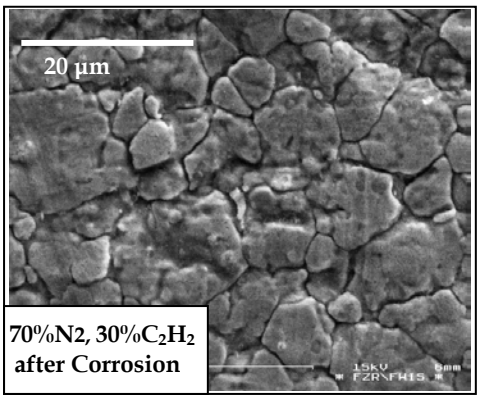
20 µm
70%N2, 30%C2H2
after Corrosion

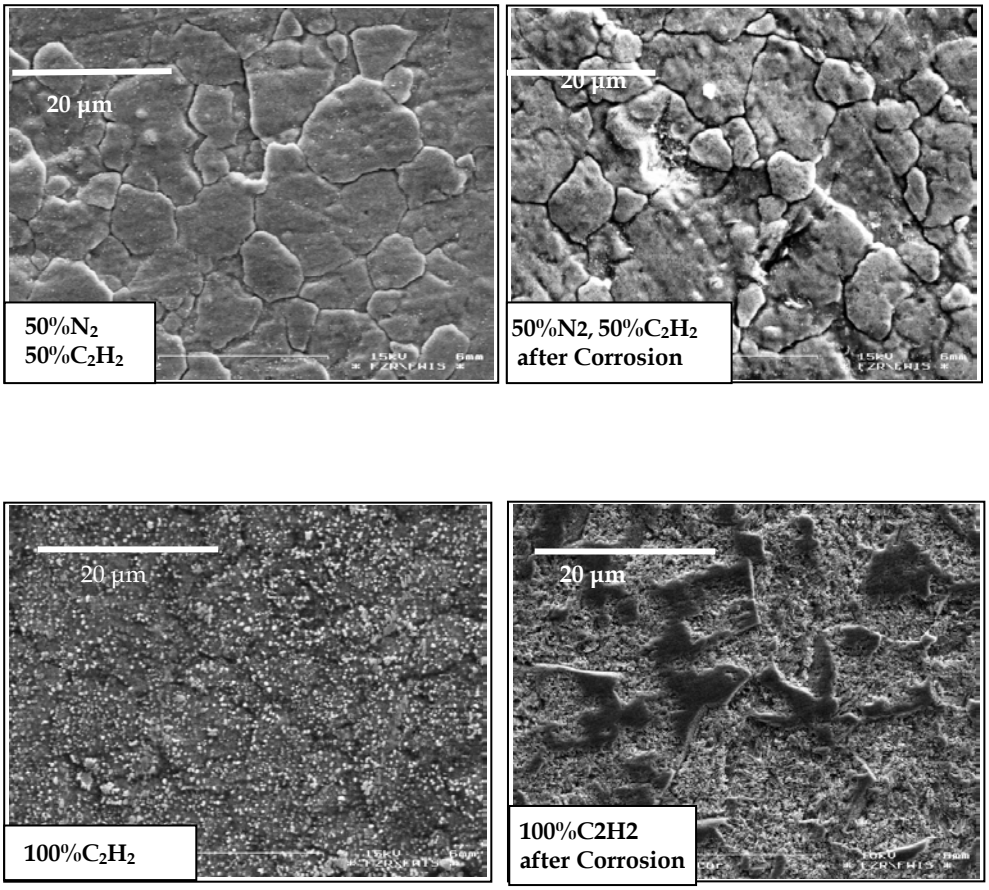

Fig. 9. SEM pictures of the surface of untreated 304 AISI and treated samples, respectively, in comparison with pictures of treated samples after corrosion test. The last image is for treated sample at 100 % C_2H_2 scanned after removing few tens nanometers from the surface.

Two distinguishable regions are observed on the surface of the samples, beside the white points and the black base. For 100% N_2, one observes a very fine white uniform deposition all over the surface. On the surface of sample treated with 100% C_2H_2 the white deposition is larger. For 50% N_2, surface fractures and little particle deposition can be seen. EDAX analysis shows that the white precipitations contain more carbon than the black ones. The elemental composition of the untreated, treated samples and selected parts was analysed by EDAX and the results are listed in Table 1. For nitrocarburizing with 50 % N_2 and 50 % C_2H_2, the nitrogen concentration is higher than that of carbon.

	N (at.%)	C (at.%)	Fe (at.%)	Cr (at.%)	Ni (at.%)
304 ASS	0	0	72.3	19.1	8
100 % N2	15.2	0	58.5	17.6	8
50 % N2	18.8	12.1	46.2	15.5	6.9
100 % C2H2	0	46	37.9	9.3	5.8

Table 1. Surface elemental composition of ASS and selected treated samples determined by EDAX.

The SEM pictures of the treated layer after corrosion test show that the corrosion occurs predominantly by bitting, intergranular or by general attack, depending on the difference of the corrosion rate of the grain boundary zones or the grain faces. This difference in rate is determined not only by the metallurgical structure and the composition of the boundary, but also by the characteristics of the corroding solution. The corrosion attack decreases with increasing the carbon content up to 30 % C_2H_2. After that the attack increases again. At 100 % N_2 the surface undergoes significant corrosion leading to visible intergranular stress corrosion cracking. The surface obtained by treatment with 100 % C_2H_2 exhibits dealloying by selective material dissolution over large surface regions. The substrate is anodic to carbon-bound region and corrodes, leaving behind a mass of carbon compound related areas. In both cases, with pure nitriding or pure carburizing, the loss of corrosion resistance is associated with the depletion of Cr in regions near the grain boundaries. That component, however, is necessary for regeneration of corrosion protective film.

These results are in accordance with those from potentiodynamic polarization curves, as shown in Fig. 8. Samples treated at 100 % N_2 or 100 % C_2H_2 corrode significantly as evidenced by their more negative corrosion potentials and high corrosion currents. Moderate nitrogen content appears to degrade the corrosion resistance insignificantly, especially for the gas ratio 70 % N_2/30 % C_2H_2.

4. Discussion

The plasma efficiency may be increased due to creation of more plasma species such as H, CH, NH, HCN or CN by adding C_2H_2 to N_2 gas during rf plasma carbonitriding. The microstructure of the modified layers depends on the pressure ratio between nitrogen and acetylene plasma gas. The nitride phases and their intensities increased by adding C_2H_2. The effect of adding acetylene has been also observed in [18] where 0.7 % of C_2H_2 was used in addition to the N_2 gas. Even though Blawert et. al. [8, 19] has observed the nitrogen and carbon expanded austenite phases nearly at the same peak positions as in our case. However, we can not ignore that at high N-content by XRD the γ_n phase can not be easily distinguished from the Fe_4N phase. Both nitride and carbide phases contribute to the improvement of the mechanical properties of the treated samples. Nitride phases (γ_n) are harder than the carbide phases (γ_c) [8]. The interplay between the temperature and gas composition might be caused by the effect of hydrogen from the acetylene gas. Compared to carbon and nitrogen the mass difference between plasma species and the ionization potential of atoms can play an important role in the resulting plasma temperature (electron

and ion temperature) which has an influence on the temperature of the substrate. In this case, the ionization potential of hydrogen is 6.4 % lower than of that nitrogen and the light hydrogen ions are easily to accelerate by the rf plasma field. These ions itself contribute to the plasma heating due to secondary electrons generation by elastic collisions with the plasma species.

Most probably, the high increase in the surface roughness, especially for the samples treated at high nitrogen content, is correlated with the increase in the sample temperature beside some physical reactions between the heavy plasma species such as CN and HCN and the surface. In a comparable study concerned with nitriding of stainless steel by plasma immersion ion implantation, the formation of expanded austenitic phase in the matrix was accompanied by a high improvement of the microhardness. However, the surface roughness increased by a factor of 4.6 and 7 at 450 °C and 520 °C, respectively [20]. Blawert et. al. [21] has attributed to the increasing in the surface roughness of treated 304-AISI samples to the sputtering surfaces caused by ion bombardment during the treatment. Even though, an increase in the substrate temperature has been observed for samples prepared at high and at pure carbon content, the surface roughness is sharply decreased. It might be due to the decrease in the physical reactions and the high amount of fine precipitations from carbon on the surface.

The decrease in the friction coefficient for samples treated at high C_2H_2 content can be attributed to the fine precipitation from carbon on the surface, which works as solid lubricant between sliding surfaces in wear experiment. After that, as the wear path increased, the effect of fine precipitation of carbon nearly disappeared. Therefore, the friction coefficient increases with the number of wear tracks. This suggestion is supported experimentally by imaging the carburized surface after removing a few hundred nanometres by a fine mechanical polishing (Fig. 9). The high number of carbon precipitations is nearly removed after polishing. Obviously, the wear behavior is influenced by the microstructure of the first sublayer which is created in dependence of the gas composition by the process of nitriding, carburizing or nitrocarburizing. Blawert [8] has reported that nitrogen expanded austenite layers are harder than those of the carbon expanded and therefore this results in smaller wear depth at low load (5 N). The role of the oxide layer is completely different in the wear behavior of untreated and treated samples. In untreated samples the oxidized wear particles lead to severe wear resulting in a high friction coefficient for the sliding of surfaces. However, for all treated samples, the oxide layer works in the opposite direction. The oxide layer of samples treated at high nitrogen content or high carbon content contains low or high amount of fine precipitations from carbon on the surface, respectively. This oxide layer acts as a lubricating layer, which prevents metal-to-metal contact, decreases the friction coefficient, reduces adhesive wear and therefore generally reduces the wear [17].

The high concentration of nitrogen detected by EDAX on the surface of the nitrocarburized sample is supported by the XRD results, which show that more nitride phases are created in the compound layer.

The solid solution phase γ_N should maintain the good corrosion resistance of stainless steel [5, 21]. But in our case, microstructure reveals that high parts of chromium nitride or chromium carbide are detected on the surface precipitated at the grain boundaries, which

are responsible for the breakdown in the corrosion resistance [20]. The degradation in corrosion resistance of the modified layers is mostly related to the concentration of CrN and CrC. It is well known that the nature of the corrosion reactions depends on the microstructure of the treated surface which controlled by gas composition and treatment temperature. Using XPS, Borges et al. [18] have recently observed a decrease in the chromium concentration on the nitride surface by adding small amount of acetylene. The authors interpreted this decrease in chromium concentration on the surface by the chemical formation of Cr-H_x (x = 1, 2) which is partly removed by the vacuum system. Former experiments involving the reaction of chromium atoms with H_2 and matrix isolation of the products have provided the spectroscopic evidence for the molecules CrH_2 and CrH [22]. In our case the intensity of CrN decreases with the increase of C_2H_2 up to 30 %, onward it increases again. This is in a good agreement with the sharp increase in the corrosion resistance of the same sample in comparison with the pure nitrided or pure carburized layer. Maybe the formation rate of the CrH_2 and CrH on the surface is higher than the precipitation rate of CrN in the grain boundaries on the surface of the sample prepared at 30 % C_2H_2. But by the increase of the substrate temperature higher than 525 ˚C, the balance in the two rates has been changed.

5. Conclusions

The gas composition has a significant influence on the microstructure of the modified layers. At nitrocarburizing, most of phases related to nitride phases (such as γ_n, Fe_2N, Fe_3N, Fe_4N and CrN) and carbide phases (such as γ_c, Fe_3C and CrN or CrC) for samples treated at high nitrogen content and high carbon content, respectively. In dependence on the gas composition ratio (N_2/C_2H_2), the sample temperatures varied from 475 ˚C to 600 ˚C. The surface roughness was found to increase as the C_2H_2 content increases up to 50 % but it decreases for higher ratios. The amount of fine precipitations of carbon on the surface is responsible for the gradually decrease in the surface roughness and friction coefficient for samples prepared at high and pure carbon content. In comparison to the untreated samples, the wear rate is reduced by more than two orders. The carbonitrided layer exhibits higher corrosion resistance in comparison to the layers obtained after pure nitriding or pure carburizing treatment. The lower content of the CrN phase leads to a good corrosion resistance. Pure nitriding samples are exposed to a strong biting corrosion surrounded by intergranular corrosion where the carburized layer is exposed to general corrosion.

6. References

[1] N. Yasumaru, Mater. Trans. 39 (1998) 1046.
[2] Y.F. Liu, J.S. Mu, X.Y. Xu, S.Z. Yang, Mater. Sci. Eng. A 458 (2007) 366.
[3] Ajit K. Roy, Vinay Virupaksha, Mater. Sci. Eng. A 452–453 (2007) 665.
[4] Jan Macák, Petr Sajdl, Pavel Kučera, Radel Novotný, Jan Vošta, Electrochim. Acta 51(2006) 3566.
[5] Z. L. Zhang, T. Bell, Surf. Eng. 1 (1985) 131.
[6] E. Menthe, K.-T. Rie, Surf. Coat. Technol. 116-119 (1999) 199.
[7] E. Richter, R. Günzel, S. Parascandola, T. Telbizova, O. Kruse, W. Möller, Surf. Coat. Technol. 128-129 (2000) 21.

[8] C. Blawert, H. Kalvelage, B. L. Mordike, G. A. Collins, K. T. Short, Y. Jirásková, O. Schneeweiss, Surf. Coat. Technol. 136 (2001) 181.
[9] F. M. El-Hossary, N. Z. Negm, S. M. Khalil, A. M. Abd El-Rahman, Thin Solid Films 405 (2002) 179.
[10] A. M. Abd El-Rahman, Surf. Coat. Technol., 205 (2010) 674-681.
[11] F. M. El-Hossary, N. Z. Negm, S.M. Khalil, A. M. Abd El-Rahman, M. Raaif, S. Maendl, Journal of Applied Physics A 99 (2010) 489-495.
[12] A. M. Abd El-Rahman, F. M. El-Hossary, T. Fitz, N. Z. Negm, F. Prokert, M. T. Pham, E. Richter and W. Moeller, Surf. Coat. Technol., 183 (2004) 268- 274.
[13] J. Takada, Y. Ohizumi, H. Miyamura, H. Kuwahara, S. Kikuchi, I. Tamura, J. Mater. Sci. 21 (1986) 2493.
[14] A. Tekin, J. Martin, B. Senpior, Journal of Material Science 26 (1991) 2458.
[15] M. Samandi, B. A. Shedden, D. I. Smith, G. A. Collins, R. Hutchings, J. Tendays, Surf. Coat. Technol. 74-75 (1995) 417.
[16] Wang Liang, Xu Bin, Yu Zhiwei, Shi Yagin, Surf. Coat. Technol. 130 (2000) 304.
[17] P. A. Dearnley, A. Namvar, G. G. A. Hibberd, T. Bell, Surface Engineering: Proceedings of International Conference PSE, DGE (1989) 219.
[18] C. F. M. Borges, S. Hennecke, E. Pfender Surf. Coat. Technol. 123 (2000) 112.
[19] C. Blawert, B. L. Mordike, G. A. Collins, K.T. Short, Y. Jiraskova, O. Schneeweiss, V. Perina, Surf. Coat. Technol. 128-129 (2000) 219.
[20] M. Samandi, B. A. Shedden, D. I. Smith, G. A. Collins, R. Hutchings, J. Tendays, Surf. Coat. Technol. 59 (1993) 261.
[21] C. Blawert, A. Weisheit, B. L. Mordike, F. M. Knoop, Surf. Coat. Technol. 85 (1996) 15.
[22] Z. L. Xiao, R. H. Hauge, J. L. Margrave, J. Phys. Chem. 96 (1992) 636.

Corrosion Resistance

Edited by Dr Shih

ISBN 978-953-51-0467-4
Hard cover, 472 pages
Publisher InTech
Published online 30, March, 2012
Published in print edition March, 2012

The book has covered the state-of-the-art technologies, development, and research progress of corrosion studies in a wide range of research and application fields. The authors have contributed their chapters on corrosion characterization and corrosion resistance. The applications of corrosion resistance materials will also bring great values to reader's work at different fields. In addition to traditional corrosion study, the book also contains chapters dealing with energy, fuel cell, daily life materials, corrosion study in green materials, and in semiconductor industry.

How to reference

In order to correctly reference this scholarly work, feel free to copy and paste the following:

A.M. Abd El-Rahman, F.M. El-Hossary, F. Prokert, N.Z. Negm, M.T. Pham and E. Richter (2012). Corrosion Performance and Tribological Properties of Carbonitrided 304 Stainless Steel, Corrosion Resistance, Dr Shih (Ed.), ISBN: 978-953-51-0467-4, InTech, Available from: http://www.intechopen.com/books/corrosion-resistance/corrosion-performance-and-tribological-properties-of-carbonitrided-304-stainless-steel

INTECH
open science | open minds

InTech Europe
University Campus STeP Ri
Slavka Krautzeka 83/A
51000 Rijeka, Croatia
Phone: +385 (51) 770 447
Fax: +385 (51) 686 166
www.intechopen.com

InTech China
Unit 405, Office Block, Hotel Equatorial Shanghai
No.65, Yan An Road (West), Shanghai, 200040, China
中国上海市延安西路65号上海国际贵都大饭店办公楼405单元
Phone: +86-21-62489820
Fax: +86-21-62489821